Oncogene (2005) 24, 4956–4964

www.nature.com/onc

The MCT-1 oncogene product impairs cell cycle checkpoint control and transforms human mammary epithelial cells

Hsin-Ling Hsu[1,2], Bo Shi[1] and Ronald B Gartenhaus*[,1,3]

[1]*Division of Hematology/Oncology, Department of Medicine, Northwestern University Feinberg School of Medicine and the Robert H Lurie Comprehensive Cancer Center of Northwestern University, Chicago, IL 60611, USA;* [2]*Division of Molecular and Genomic Medicine, National Health Research Institutes, 128 Yen-Chiu-Yuan Road, Sec. 2, Taipei 115, Taiwan;* [3]*University of Maryland Greenebaum Cancer Center, 9-011 BRB, 655 West Baltimore Street, Baltimore, MD 21201, USA*

Multiple copies in T-cell maligancy (MCT-1) is a putative oncogene initially identified in a human T-cell lymphoma. Forced expression of MCT-1 has recently been shown to induce cell transformation and proliferation, as well as to activate survival-related PI-3K/AKT pathways protecting cells from apoptosis. MCT-1 protein is stabilized in response to DNA damage. The impact of MCT-1 overexpression on DNA damage response remains unknown. Here, we show that MCT-1 deregulates cell cycle checkpoints. The phosphorylation of genomic stabilizers H2AX and NBS1 are enhanced in MCT-1-overexpressing cells. Forced expression of MCT-1 significantly increases the number of DNA damage-induced foci involving γ-H2AX and 53BP1. In MCT-1-overexpressing cells, the proportion of S-phase cell population is preferentially increased after exposure to γ-irradiation compared to controls. Knockdown of endogenous MCT-1 using an siRNA approach attenuates the H2AX phosphorylation and the G1/S checkpoint defect. Furthermore, MCT-1 is capable of transforming immortalized human mammary epithelial cells and promoting genomic instability. These data shed light on the role of MCT-1 in the cellular response to DNA damage and its involvement in malignant transformation.
Oncogene (2005) **24,** 4956–4964. doi:10.1038/sj.onc.1208680; published online 9 May 2005

Keywords: transformation; cell cycle

Introduction

Double-stranded DNA breaks (DSBs) induced by exogenous or endogenous DNA-damaging agents are potentially lethal forms of stress as they disrupt genomic integrity. Irreparable DNA damage has the potential to transform cells if these genetic alterations lead to loss of tumor suppressors or activation of oncogenes. Predisposition to tumor formation is increased further by the propagation of genomic defects due to abrogation of cell cycle checkpoint controls. Surveillance of the genome structure by proper activation of DNA –damage-repair complex is an essential molecular mechanism to suppress tumor formation.

In addition to maintaining nucleosome architecture, histone H2AX is an immediate target of damage-activated ATM and DNA-PK kinase (Paull *et al*., 2000; Burma *et al*., 2001; Stiff *et al*. 2004). Rapid phosphorylation of H2AX (γ-H2AX) by activated kinase assembles the transient nuclear repair foci in close proximity to the DNA lesion sites. The number of γ-H2AX foci correlates well with the number of DSBs, and the disappearance of γ-H2AX foci matches well with the kinetics of DNA repair (Rogakou *et al*., 1999). While γ-H2AX is not the primary signal required for the initial recruitment of the individual repair proteins, such as NBS1, 53BP1, and BRCA1 to the damaged chromatin, it is required to maintain repair complexes that have accumulated in the vicinity of DSBs (Celeste *et al*., 2003a, b). Murine models have demonstrated that H2AX gene disruption led to genomic instability associated with radiation-hypersensitivity and DNA repair defects (Bassing *et al*., 2002; Celeste *et al*., 2002). Extensive studies in mammals indicate that the gene dosage of H2AX is critical for suppression of transforming chromosomal translocations and subsequent tumor formation (Bassing *et al*., 2002; Celeste *et al*., 2003a, b). Although a number of damage checkpoint molecules colocalize with the γ-H2AX damage-repair complex, the precise components of the damage-repair foci and their biological significance in differential temporal/spatial assembly are still unclear (Chen *et al*., 2000; Petersen *et al*., 2001; Celeste *et al*., 2003a, b; Ward *et al*., 2003). The ATM-dependent checkpoint molecule 53BP1 forms nuclear DNA damage foci that are constitutively activated in human cancer cell lines. The 53BP1 protein plays an important role in stabilization of genomic structure and has functional interaction of H2AX in DNA damage response (Ditullio *et al*., 2002; Fernandez-Capetillo *et al*., 2002; Morales *et al*., 2003). Furthermore,

*Correspondence: RB Gartenhaus, University of Maryland Greenebaum Cancer Center, 9-011 BRB, 655 West Baltimore Street, 22 South Greene Street, Baltimore, MD 21201, USA;
E-mail: rgartenhaus@som.umaryland.edu
Received 17 December 2004; revised 10 February 2005; accepted 3 March 2005; published online 9 May 2005

γ-H2AX is also detected in naturally occurring DSBs, such as DNA replication, chromosomal recombination, V(D)J recombination, apoptosis, and senescence processes, indicating its broad biological functions (Chen *et al*., 2000; Ward and Chen, 2001; Furuta *et al*., 2003).

The candidate oncogene, designated multiple copies in T-cell maligancy (MCT-1), was initially identified in the HUT 78 T-cell lymphoma line (Prosniak *et al*., 1998). Constitutive expression of MCT-1 results in hyperproliferative signal(s) associated with decreased cell doubling time, shortened G1 transition, increased cyclin D1 and CDK4 activities (Dierov *et al*., 1999). MCT-1's oncogenic potential is further supported by its transforming capacity in NIH3T3 cells (Prosniak *et al*., 1998). Recently, we reported that a panel of primary human lymphoma cells expressed significantly higher levels of MCT-1 protein than normal lymphocytes (Shi *et al*., 2003). Furthermore, we showed that increasing MCT-1 levels strongly enhanced the phosphorylation of AKT at Ser473 residue and increased cell survival by preventing apoptotic events. Moreover, MCT-1 is stabilized in response to irradiation and other DNA-damaging agents by post-translational mechanism(s) unknown at present (Herbert *et al*., 2001). Here, we present novel effects of constitutively expressed MCT-1 on the cellular DNA damage responses; including deregulation of the DNA damage cell cycle checkpoint and hyperphosphorylation of genome surveillance factors. The combined effects of genome destabilization and enhanced cell proliferation/survival signaling strongly support the involvement of MCT-1 protein in malignant cell transformation.

Results and discussion

MCT-1 impairs cell cycle checkpoint control

DNA damage checkpoint controls are critical for maintaining genomic stability. Cells that are transformed by oncogenes frequently escape from genomic damage surveillance (Malumbres and Barbacid, 2001). To examine the consequences of forced expression of MCT-1 on cellular response to DNA damage, the human breast tumor cell line MCF-7 was transduced either with the retroviral vector encoding full length of MCT-1 or with the empty vector. Under G418 selection for 2 weeks, pools of drug-resistant cells were selected or individual stable clones were expanded. Asynchronously cycling MCF-7 cells expressing MCT-1 and the empty vector were exposed to a lethal dose (10 Gy) of ionizing radiation (IR). At different time intervals postirradiation, the percentages of cells at G1, S, and G2–M phase of cell cycle were analysed by flow cytometry (FACS) (Figure 1a). The ratio of S/G1 after IR treatment at each time point was quantified for the respective cell populations from three independent experiments (Figure 1b). Notably, at 5 h (hours) postirradiation, the S/G1 ratio of cells expressing MCT-1 was twofold (1.84/0.89) greater than vector control cells (Figure 1a–c), suggesting that an increasing amount of ectopic MCT-1 cells were entering S-phase stage. At 10 h postirradiation, this enhanced S-phase population was attenuated, as the S/G1 ratio of MCT-1-expressing cells was equivalent to vector control cells. G2/G1 ratio in MCT-1-expressing cells did not show a significant increase as compared to the control group.

The increasing level in S/G1 ratio suggests that the overexpression of MCT-1 may bypass G1 checkpoint and promote S-phase progression in MCF-7 cells. To assay the incorporation of bromdeoxyuridine (BrdU) into newly synthesized DNA following γ-irradiation, subconfluent cultured MCT-1-overexpressing and vector control cells were exposed to 10 Gy of γ-irradiation ($+$IR), and subsequently cultured in complete medium supplemented with BrdU. At 4 h postirradiation, the amount of DNA-replicating cells was quantified by the immunostaining of nuclei with FITC-conjugated anti-BrdU Ab followed by confocal fluorescent microscopy and flow cytometric analysis (Figure 1d, e). Consistent with an S/G1 ration increasing phenotype, the percentages of cells incorporating BrdU were elevated in the MCT-1-overexpressing group (40%). However, the control group demonstrated a more intact G1 checkpoint, BrdU-positive cells (15%) were proportionally reduced after irradiation. In addition, employing FACS analysis, we identified a greater population (>2-fold) of BrdU incorporation in MCT-1-overexpressing cells that bypassed G1 checkpoint.

MCT-1 hyperactivates DNA damage signaling pathway

Using immunofluorescence microscopy, we demonstrated that ectopically expressed MCT-1 was prefer entially localized to the interphase nuclear compartment and mitotic chromosomes in MCF-7 cells (Figure 2a), consistent with the subcellular nuclear fractionation data (Figure 2b). Further analysis on the impact of MCT-1 in DNA damage signaling cascades revealed that autophosphorylation of ATM (Ser1981) and phosphorylation of NBS1 (Ser343) mediated by ATM kinase were induced approximately twofold, while phospho-H2AX (Ser136) has more than a 10-fold induction (Figure 2c). This raises the possibility that other PI-3K-related kinase, such as ATR or DNA-PKcs, may be involved in H2AX phosphorylation (Ward and Chen, 2001; Stiff *et al*., 2004), in addition to ATM.

MCT-1 induces H2AX phosphorylation and DNA damage foci formation

Next, we examined whether overexpression of MCT-1 affects genome surveillance signaling pathways. The γ-irradiation-induced phosphorylation of H2AX on Ser139 site (γ-H2AX) was immediately observed and was significantly augmented in MCT-1-overexpressing cells in an irradiation dose-dependent manner (Figure 3a). Examination of the kinetics of γ-H2AX induction revealed that, even prior to irradiation, γ-H2AX levels were already detectable in

a C : control M: MCT-1 over-expression

cell types	cell cycle phases (%) G1	S	G2	S/G1 ratio (fold)	G2/G1 ratio (fold)
C0	46.62	33.87	19.51	0.71 (1)	0.4 (1)
C5	49.44	31.49	19.08	0.64 (0.89)	0.38 (0.95)
C10	37.13	32.34	30.53	0.87 (1.21)	0.82 (2.05)
C24	52.12	5.89	41.90	0.11 (0.15)	0.8(2)
M0	48.61	32.74	18.66	0.67 (1)	0.38 (1)
M5	35.99	44.31	20.09	1.23 (1.84)	0.56 (1.47)
M10	36.17	32.41	31.42	0.89 (1.33)	0.87 (2.29)
M24	49.37	7.07	43.56	0.14 (0.21)	0.88 (2.32)

b

S/G1 Ratio	Mean	SE
C0	1	0
C5	0.88	0.03
C10	1.21	0.02
C24	0.14	0.01
M0	1	0
M5	1.85	0.04
M10	1.35	0.07
M24	0.18	0.02
G2/G1 Ratio	**Mean**	**SE**
C0	1	0
C5	0.95	0.02
C10	2.06	0.03
C24	1.98	0.03
M0	1	0
M5	1.42	0.05
M10	2.38	0.15
M24	2.25	0.18

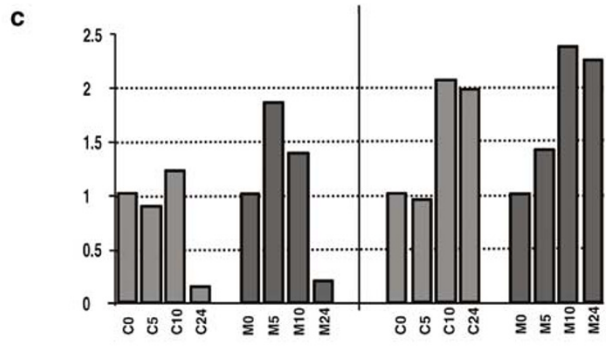

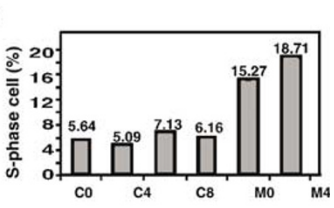

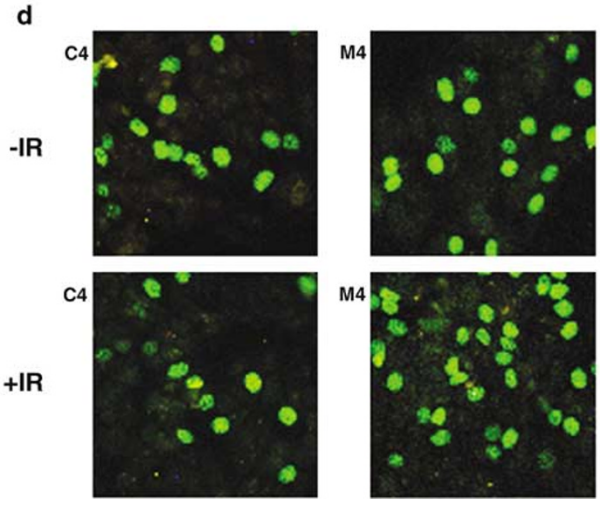

Figure 1 Overexpression of MCT-1 deregulates cell cycle checkpoint. (**a**) FACS analysis of cell cycle profiles. In MCT-1 and empty vector-transfected MCF-7 cells, the percentages of cells at different phases of cell cycle in response to γ-irradiation (10 Gy) was examined. According to the cell population situated at the G1, S, G2/M phases, the ratio of S/G1 at each time interval (0, 5, 10, 24 h) was calculated. The ratio of S/G1 and G2/G1 prior to damage treatment was normalized as 1. The increasing fold of S/G1 and G2/G1 ratio between each time point were compared. (**b**, **c**) The data and histogram represent the average of S/G1 and G2/G1 increasing folds from triplicate experiments. Standard error (s.e.). A significant elevation of S/G1 ratio in MCT-1-expressing cells was observed after γ-irradiation treatment for 5 h, indicating that more ectopic MCT-1-expressing cell populations are entering S-phase stage than control cells. (**d**, **e**) DNA replicating cells. MCT-1-overexpressing MCF-7 cells versus vector controls were cultured with complete medium and BrdU. In comparison with the control cells after irradiation exposure for 4 h, the amounts of BrdU-positive cells were markedly increased in the MCT-1-overexpressing cells as detected by immunofluorescent staining analysis (**d**). The increased BrdU incorporation was quantified by FACS analysis and demonstrated concordant results. DNA replicating cells are approximately 2–3-fold greater in MCT-1-expressing cells than the control cells (**e**)

MCT-1-overexpressing cells. We also observed damage-induced γ-H2AX occurring rapidly and persisting for at least 24 h in MCT-1-overexpressing cells, whereas γ-H2AX was only transiently present in control cells (Figure 3b). To confirm that prolonged γ-H2AX duration by MCT-1 is dependent upon an activated PI-3K-related kinase, various concentrations of the specific PI-3K inhibitor Wortmannin (Wort.) were added to the cultures prior to irradiation treatment. The elevated levels of γ-H2AX were effectively suppressed at 50 μM in both MCT-1 and control cells (Figure 3c), further linking MCT-1 activity with a

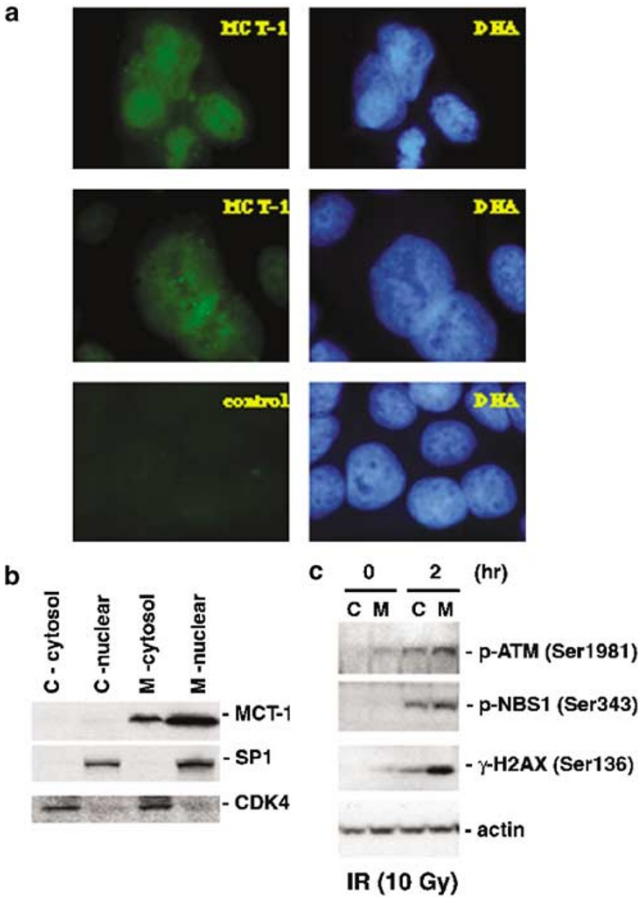

Figure 2 MCT-1 stimulates ATM downstream events. (**a**) Immunofluorescent staining pattern demonstrates that the overexpressed MCT-1 protein is predominantly at interphase nucleus and colocalized with mitotic chromosomes. (**b**) Subcellular distribution of ectopically expressed MCT-1 indicates that MCT-1 is more abundant in nucleoplasm than cytoplasm. The distributions of nuclear SP1 and cytosolic CDK4 proteins are used as subcellular fraction controls. (**c**) ATM autophosphoryaltion at Ser1981 and ATM-activated phosphorylation of NBS1 (Ser343) are modestly induced. H2AX phosphorylation at Ser136 is strongly augmented by the ectopic expression of MCT-1 either before or after DNA damage

functional PI-3K-related kinase pathway. Consistent with MCT-1's action in MCF-7 breast cancer cells, the phospho-Ser139 H2AX was also clearly increased in nonirradiated EC155 lymphoma cells that overexpressed MCT-1 (Figure 3d). The γ-H2AX induction by MCT-1 apparently is not restricted to one tissue type.

The phosphorylation of H2AX at Ser139 is correlated with nuclear damage-repair foci formation (Rogakou *et al*., 1999). We monitored the assembly of γ-H2AX foci in cells using immunofluorescent microscopy (Figure 4a), a greater number of distinct γ-H2AX foci were visualized in MCT-1-expressing cells compared with control cells at the indicated time intervals. The most significant difference was noted at 2 h postirradiation, an interval when vigorous DNA repair processes are activated (Wang *et al*., 2001). At 7 h postirradiation, γ-H2AX foci were aggregated into larger irregular granules in MCT-1-expressing cells, while the number of foci was apparently reduced and exhibited dispersed smaller punctuate dots in the control group. DSB repair seems to be potentiated in MCT-1-inducing cells; this phenomenon could potentially produce tumorigenic chromosome translocations as previously described (Aten *et al*., 2004). Intriguingly, some of the MCT-1-expressing cells displayed a remarkably strong staining pattern of γ-H2AX (indicated by arrowheads) that may represent robust DNA replication stress or genomic defects occurring, when MCT-1 is highly abundant. Furthermore, the number and the intensity of 53BP1 nuclear damage foci, which has been shown to have functional interactions with H2AX and to be involved in genome stabilization (Ditullio *et al*., 2002; Morales *et al*., 2003), were strongly increased in the presence of elevated MCT-1 (Figure 4b, M0 and M1). This large number of 53BP1 foci developed in MCT-1-overexpressing cells may be related to 53BP1 constitutive activation in human cancer cells as described.

Knockdown of MCT-1 restores G1 checkpoint and decreases γ-H2AX levels

We knocked down endogenous MCT-1 by a retrovirally delivered small interfering dsRNAs (siRNA) in order to directly examine the biological roles of endogenous

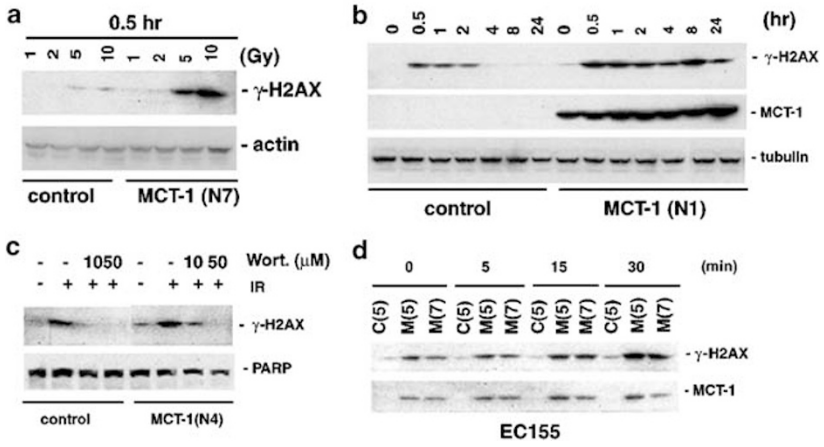

Figure 3 MCT-1 hyperactivates H2AX phosphorylation. (**a**) The phosphorylation status of H2AX at Ser139 residue (γ-H2AX) was examined as an early DNA damage event. MCF-7 cells transfected with (N7) or without (control) MCT-1 expression vector were irradiated with varying doses (1–10 Gy) for 0.5 h. A specific antibody directly against phospho-Ser139 H2AX monitored the appearance of γ-H2AX. Forced-expression of MCT-1 induces γ-H2AX in a radiation dose-dependent manner. (**b**) MCF-7 cells exposed to 10 Gy of irradiation were subsequently chased for the indicated periods of time. A highly sustained γ-H2AX induction was observed in MCT-1-overexpressing cells (N1), while γ-H2AX was only transiently expressed in control cells. The increased stabilization of MCT-1 was detected at 1–2 h postirradiation. (**c**) Prior to γ-irradiation treatment, MCF-7 cells were preincubated with a PI-3K inhibitor Wortmannin at various concentrations (0, 10, and 50 μM) for 3 h. Wortmannin effectively inhibits the induction of γ-H2AX in a dose of 50 μM. (**d**) EC155 lymphoma cell lines overexpressing MCT-1 (M5, M7) were treated with γ-irradiation (10 Gy). As compared to the EC155 control cells (C5), γ-H2AX was also highly induced by MCT-1. The increased levels of γ-H2AX were noted even before damage exposure

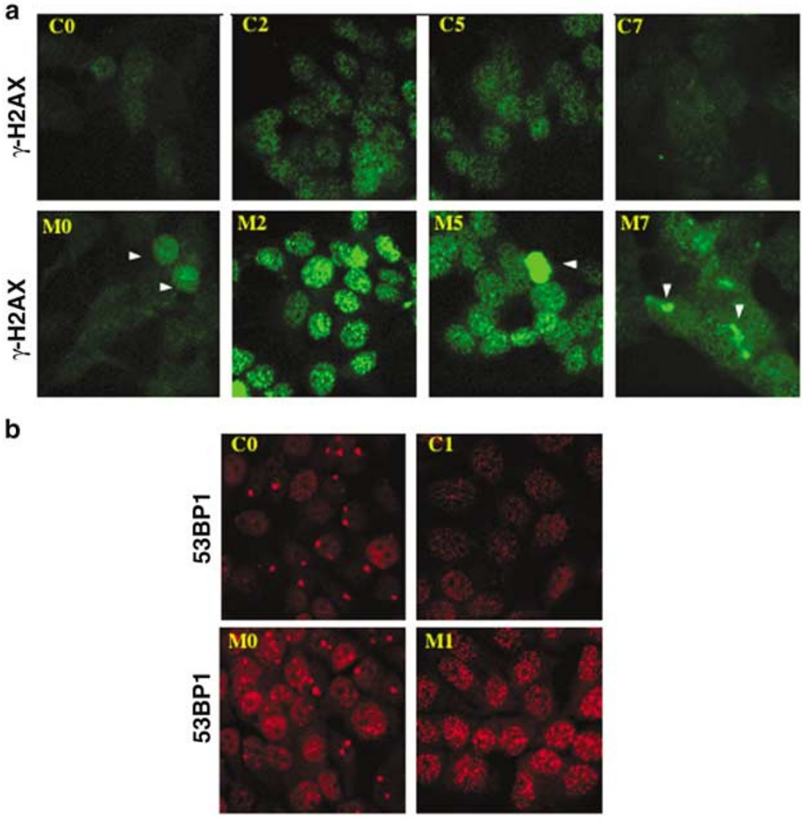

Figure 4 MCT-1 induces γ-H2AX and 53BP1 repair foci formation. (**a**) MCF-7 cells expressing MCT-1 (M0–M7) or vector control (C0–C7) were grown on slide chambers followed by irradiation with 10 Gy. At discrete time intervals, nuclear damage-repair foci of γ-H2AX were immunodetected with the phospho-Ser139 H2AX antibody and then examined with confocal microscopy (× 40). In MCT-1-overexpressing cells, the occurrences of γ-H2AX foci are strikingly increased and persist at 7 h post-treatment compared to the less distinct foci detected in control group. (**b**) The formation of nuclear 53BP1 foci are also dramatically enhanced in MCT-1-overexpressing cells before (M0) or 1 h postirradiation treatment (M1) as compared to nonirradiated (C0) or irradiated control cells (C1)

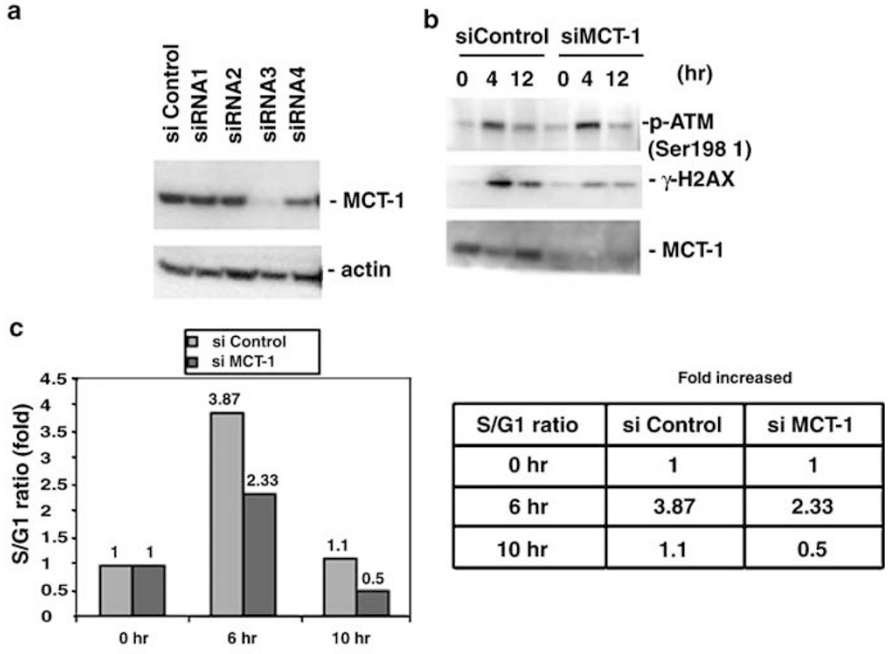

S/G1 ratio	si Control	si MCT-1
0 hr	1	1
6 hr	3.87	2.33
10 hr	1.1	0.5

Figure 5 Knock down MCT-1. (**a**) Using a retroviral siRNA expression vector, endogenous MCT-1 protein expression is virtually eliminated from parental MCF-7 cells by the siRNA-3 construct. (**b**) Postirradiation, the damage-induced phosphorylation of ATM and H2AX were examined. MCT-1 knockout (siRNA-3) reduces γ-H2AX levels but not phospho-ATM. (**c**) The significant reduction of S/G1 ratio in MCT-1 knockout cells indicated that DNA damage checkpoint effect was increased. The data are representative of at least three independent experiments

MCT-1 in response to DNA damage. Stable MCT-1 knockdown cells were confirmed by Western blotting (Figure 5a). Following DNA damage, MCT-1 knockdown decreased H2AX phosphorylation at Ser136; however, MCT-1 deficiency did not significantly alter ATM autophosphorylation (Figure 5b). The data suggest that MCT-1 modulates γ-H2AX occurrence through a pathway that is not entirely dependent on ATM autophosphorylation.

In contrast to MCT-1 ectopic expression (Figure 1), the MCT-1 knockdown (siMCT-1) cells were more effectively arrested at G1–S boundary in comparison with control RNAi knockdown (siControl) cells in response to DNA damage as shown by the reductions of S/G1 ratio (Figure 5c). The data indicates that MCT-1 plays an important role in cell cycle regulation, while MCT-1 overexpression deregulating G1 checkpoint and DNA damage-repair signaling responses (Figures 1–4).

Constitutive expression of MCT-1 induces cellular transformation

Anchorage-independent growth is one of hallmarks of malignant cell transformation that correlates well with neoplasia (Kang and Krauss, 1996). To further examine if MCT-1 induces immortalized primary human mammary epithelial cell transformation, we analysed anchorage-independent colony-forming capacity of MCF-10A cells that were retrovirally transduced with V5-tagged MCT-1 or an empty vector. Under Neomycin (G418) selection for 2 weeks, pools of drug-resistant cells were examined for the expression of V5-MCT-1 (Figure 6).

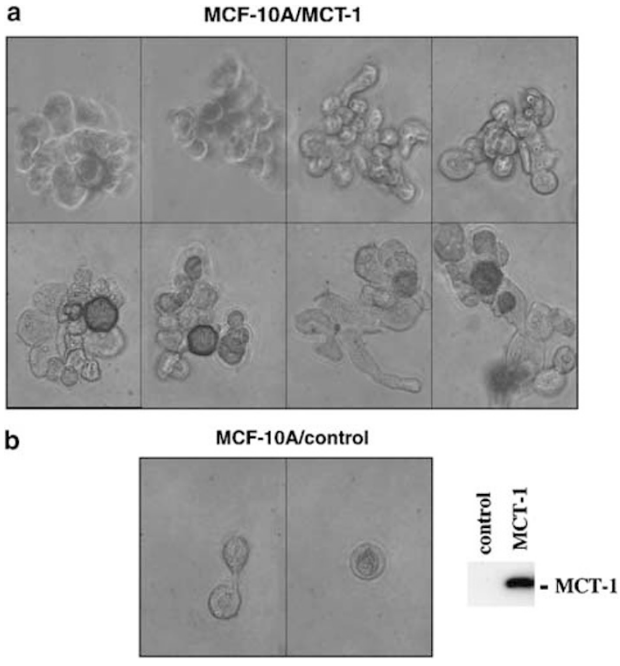

Figure 6 MCT-1 overexpression transforms immortalized MCF-10A human mammary epithelial cells. MCF-10A cells overexpressing MCT-1 (**a**) or vector control (**b**) were assayed for anchorage-independent growth. After culturing for 12 weeks, colony formation on soft agar was examined under phase-contrast microscopy ($\times 40$). As shown here, MCT-1-overexpressing cells exhibit anchorage-independent colony formation, whereas vector-transfected control cells are not capable of colony formation

After plating MCT-1 and vector-transfected MCF-10A cells onto soft agar containing appropriate culture medium, colony formation was monitored for 12 weeks. Approximately 35% of MCT-1-transfected MCF-10A cells formed multicellular colonies and exhibited irregular cellular morphology (Figure 6a). The control MCF-10A cells retained a normal phenotype and did not establish colonies (Figure 6b).

Our studies provide evidence that the MCT-1 oncogene transforms human breast epithelial cells and deregulates DNA damage-signaling pathway. We present data here that overexpression of MCT-1 increases S/G1 ratio and DNA replication frequency when compared to irradiated control cells. ATM-dependent, damage-induced phospho-modifications of genome surveillance factors, such as H2AX, BRCA1, and NBS1 are appreciably augmented in MCT-1-overexpressing background. However, the molecular basis by which MCT-1 deregulates the DNA damage-signaling cascade remains unclear at present. MCT-1 is a target for CDC2 and MAPK kinase *in vitro* (data not shown) and co-localized with mitotic chromosomes (Figure 2a), suggesting that MCT-1 may be in close proximity with genomic materials and involved in cell cycle regulation. Identifying the specific manner in which MCT-1 interacts with DNA damage and cell cycle signaling cascade is an area of active investigation.

Following cellular irradiation, rapid induction of γ-H2AX is transiently observed and then gradually diminished as DNA breaks are repaired. However, MCT-1 prolongs the duration of H2AX phosphorylation and the presence of nuclear damage-repair foci, a phenomenon that is also found in E7 oncoprotein-transformed cells in which E7 increases both γ-H2AX expression and genomic instability (Duensing and Munger, 2002). Augmented H2AX phosphorylation profile could be partly due to constitutively activated ATM and other PI-3K family kinases, ATR or DNA-PK, through an unknown mechanism involving MCT-1 activity. Alternatively, MCT-1 may promote DNA replication process, which also potentially leads to H2AX hyperphosphorylaton. Supporting evidence for the second hypothesis is the recent report demonstrating that expression of proliferating cell nuclear antigen (PCNA), the central component of DNA replication fork, is increased by MCT-1 overexpression (Shi *et al*., 2003).

A normal cell must overcome multiple self-protective mechanisms in order to become cancerous (Hahn and Weinberg, 2002). Radiation-resistant tumor cells override damage-checkpoints and continue to proliferate despite the accumulation of genomic defects. Several lines of evidence exist in support of MCT-1 being considered a *bona fide* oncogene; MCT-1-overexpressing cells bypass a G1 phase checkpoint safeguard (Figure 1), deregulate biochemical/cellular responses to DNA damage (Figures 2–5) and ultimately lead to malignant cell transformation (Figure 6). MCT-1 overexpression enhances the signaling cascade of ATM and augments nuclear damage foci assembly (Figures 2–4).

Functional amplification of MCT-1 not only stimulates growth/survival associated with enhanced phosphorylation of AKT at Ser 473 and elevated CDK activity (Dierov *et al*., 1999; Shi *et al*., 2003) but also perturbs DNA damage responses. The impaired function of G1 checkpoint may contribute to genome-defective cellular transformation in MCT-1-overexpressing cells. MCF-10A mammary epithelial cells overexpressing MCT-1 produce anchorage-independent colonies in soft agar (Figure 6), corroborating our prior published data using NIH 3T3 cells and enhances the cell proliferation and survival signaling pathways (Prosniak *et al*., 1998; Dierov *et al*., 1999; Shi *et al*., 2003). The use of MCF-10A cells as our model system provides an important tool for the investigation of molecular and biochemical changes acquired during progression of human breast neoplasia. Elucidating the mechanisms of MCT-1 on DNA damage-checkpoints may shed additional light on tumor development and progression.

Materials and methods

Antibodies and reagents

The antibodies recognizing H2AX pS139 (Upstate Biotechnology); NBS1 pS343 (Cell Signaling); SP1 (Santa Cruz); ATM pS1981, 53BP1 (Novus); and V5-epitop (Invitrogen) were purchased. Anti-MCT-1 rabbit antibody was generated against synthetic peptide (a.a. 72–88) (Zymed). The chemical reagents Wortmannin (Calbiochem) and Bleomycin (Gensia-Sicor Pharmaceuticals, Inc.) were purchased.

Plasmid constructions

The coding sequence of full length of MCT-1 was amplified from total RNA of Jurkat cells. The forwarding primer CACCATGTTCAAGAAATTTGATGAA and reversing primer TTTATATGTCTTCATATGCCACAGCC were used for PCR amplification of MCT-1-coding region. The MCT-1 PCR product was directly cloned into the TOPO-cloning sites of pcDNA3.1/V5-Histidine tag vector (Invitrogen) to generate the recombinant construct containing MCT-1 coding region fused with V5 and histidine tag at C-terminal. To further subclone full-length MCT-1 into a retroviral vector pLXSN, the pcDNA3.1-MCT-1-V5-Histidine plasmid was again PCR amplified using the forward primer of 5′-TAGAATTCAC CATGTTCAAGAAATTTGAT-3′ and reverse primer 5′-GGTTAACAGCGGGTTTAAACTCAAT-3′. After digesting with *Eco*RI and *Hpa*I, the MCT-1-V5-Histidine cDNA fragment was constructed into *Eco*RI and *Hpa*I cloning sites of retroviral expression vector pLXSN (Clontech). The pLXSN empty vector and pLXSN-MCT-1-V5-Histidine were transfected into a packaging cell line, PT67. Recombinant retroviral vector were packaged into infectious, replication-incompetent particles, and the culture media that containing viral particles were collected for cellular transfection.

Cell culture and transfection

Human breast cancer cell line MCF-7 was grown and maintained in RPMI medium supplemented with 10% fetal bovine serum (FBS), 100 U/ml Penicillin, and 100 μg/ml Streptomycin. Human nontransformed mammary epithelial

cells MCF-10A were grown in RPMI medium supplement with 10% horse serum, 100 U/ml Penicillin, 100 μg/ml Streptomycin, 20 ng/ml EGF, 0.5 μg/ml Hydrocortisone (Calbiochem), 100 ng/ml Cholera toxin (Calbiochem), and 10 μg/ml Insulin (Sigma). The cultures were propagated and replaced with fresh medium every 3 days to keep them at subconfluency. The retroviral particles contaning media were incubated with the cells for 24 h, replenished with fresh medium, and then kept under neomycin G418 (400 μg/ml) selection for 2 weeks. Stable clones and mass cultures were evaluated by V5-tagged MCT-1 expression and maintained with the growth essential medium containing 100 μg/ml of G418.

Cell transformation assay

To perform anchorage-independent assays, approximately 500 cells of MCF-10A were resuspended in RPMI medium containing 0.3% agarose and growth essential factors as described above, then overlayed onto 0.6% agarose containing growth essential components. Cells were replenished with fresh medium every 4 days. The percentage of multicellular colonies were examined under microscope and quantified after 12 weeks.

RNA interference (RNAi) system

The RNAi-ready pSIREN-RetroQ vector (BD Biosciences, Clontech) was cloned with the annealed oligonucleotides encoding MCT-1 siRNA (small interfereing dsRNA). Following the design recommendations of the manufacturer (BD Biosciences, Clontech), we designed four different siRNA oligonucleotides ranging from coding sequence of MCT-1 gene: NT324-344 (siRNA-1); NT352-372 (siRNA-2); NT503-523 (siRNA-3); NT667-687 (siRNA-4). The negative control siRNA annealed oligonucleotide (NT) was provided by the manufacturer.

Flow cytometry analysis (FACS)

At different time intervals, irradiated cells were harvested and PBS washed onced prior to fixation with 70% ethanol for 2 h or stored at -20°C. Fixed cell samples were PBS washed, recovered by centrifugation, and resuspended in 1 ml of PBS buffer containing 0.1% Triton (Sigma), 0.2 mg/ml DNase-free RNase A (Sigma), and 0.1 mg/ml of DNA dye propidium iodide (PI) (Sigma) at 37°C for 15 min. The cell populations at different phases of cell cycle were evaluated by flow cytometry (Beckman Coulter, Epics XL-MCL).

Cellular irradiation, cell extracts preparation, and immunoblotting

Cells were irradiated by Gammacell 40 Caesium 137 irradiation unit (Atomic Energy of Canada). DNA damaged-induced or noninduced cells were harvested at the indicated time, lysates were prepared by incubation cells with Cytobuster protein extraction reagent (Novagen) on ice for 15 min. The extracts were clarified by centrifugation at 4°C for 15 min. Cytoplasmic and nuclear extracts were prepared stepwise using the NE-PER nuclear and cytoplasmic extraction reagents (PIERCE Biotechnology) according to the manufacturer's instructions. Protein samples (100 μg) were heat-denatured with NuPAGE LDS sample buffer (Invitrogen) and NuPAGE reducing agent (Invitrogen), resolved by 4–12% Bis/Tris NuPAGE gel (Invitrogen), and transferred onto Hybond-C extra membrane (Amersham Biosciences). The membrane was sliced into panels according to molecular weight and simultaneously probed with the indicated antibodies. After hybridizing with HRP-conjugated sheep anti-mouse IgG or donkey-anti rabbit IgG (Amersham Biosciences), the immunoreacted proteins were visualized by ECL plus Western Blotting detection reagents (Amersham Biosciences) followed by autography. To reprobe the proteins on the same membrane, the immunoreacted signals were stripped by a Restored Western Blot Stripping Buffer (PIERCE Biotechnology).

BrdU incorporation analysis

Exponentially growing MCF-7 cells were grown onto slide chambers for 24 h. Cells were exposed to ionizing radiation and cultured with the fresh medium (10% FBS) containing 10 μM of BrdU (bromodeoxyuridine) supplied from BrdU flow kit (BD Biosciences Pharmingen). Cell samples were processed based on the instruction manual. Briefly, the cells were washed once with PBS, fixed/permeabilized with Cytofix/Cytoperm buffer, treated with Cytoperm Plus Buffer, refixed with Cytofix/Cytoperm buffer, treated with DNase, and then stained with FITC-conjugated anti-BrdU antibody. BrdU incoporated cells were examined by confocal micropscopy and FACS analysis.

Immunofluorescence microscopy

To detect DNA damge-repair foci, cells were cultured onto slide chambers for 24 h before γ-irradition exposure. At the times indicated, damage-treated or nontreated cells were under 3.5% of formaldehyde/PBS fixation for 15 min at room temperature followed by permeabilization with ice-cold acetone for 3 min at -20°C. The antibodies recognizing γ-H2AX and 53BP1 were incubated with cell samples for 2 h at room temperature. After triple washing with PBS, the samples were reacted with Alexa 488-coupled goat-anti mouse or Alexa-conjugated 543 goat-anti rabbit secondary antibodies (Molecular Probes) for 1 h at room temperature and protected from light exposure. Confocal section images were obtained with a Zeiss LSM 510 laser confocal microscope under sequential scanning. To compare the intensity of immunofluorescent signals, the parallel Confocal images were obtained under the same profile and the representive data from three independently performed experiments are shown here.

Examination of the subcellular localization of the overexpressed MCT-1, MCF-7 cells were cultured onto slides and then immunostained with ant-V5 mAb follwed by reaction with FITC-labeled goat-anti mouse secondary antibody (Molecular Probes).

Acknowledgements
We thank Dr V Graig Jordan and Dr Yossi Shiloh for helpful discussions and providing reagents, and Anne Croisetiere and Dr Bin Chen for technical support. A Merit Review Award from the Department of Veterans Affairs (RBG) and Avon Foundation Pilot Project Award (RBG) supported this work.

References

Aten JA, Stap J, Krawczyk PM, van Oven CH, Hoebe RA, Essers J and Kanaar R. (2004). *Science*, **303,** 92–95.

Bassing CH, Chua KF, Sekiguchi J, Suh H, Whitlow SR, Fleming JC, Monroe BC, Ciccone DN, Yan C, Vlasakova

K, Livingston DM, Ferguson DO, Scully R and Alt FW. (2002). *Proc. Natl. Acad. Sci. USA*, **99,** 8173–8178.

Burma S, Chen BP, Murphy M, Kurimasa A and Chen DJ. (2001). *J. Biol. Chem.*, **276,** 42462–42467.

Celeste A, Difilippantonio S, Difilippantonio MJ, Fernandez-Capetillo O, Pilch DR, Sedelnikova OA, Eckhaus M, Ried T, Bonner WM and Nussenzweig A. (2003a). *Cell*, **114,** 371–383.

Celeste A, Fernandez-Capetillo O, Kruhlak MJ, Pilch DR, Staudt DW, Lee A, Bonner RF, Bonner WM and Nussenzweig A. (2003b). *Nat. Cell Biol.*, **5,** 675–679.

Celeste A, Petersen S, Romanienko PJ, Fernandez-Capetillo O, Chen HT, Sedelnikova OA, Reina-San-Martin B, Coppola V, Meffre E, Difilippantonio MJ, Redon C, Pilch DR, Olaru A, Eckhaus M, Camerini-Otero RD, Tessarollo L, Livak F, Manova K, Bonner WM, Nussenzweig MC and Nussenzweig A. (2002). *Science*, **296,** 922–927.

Chen HT, Bhandoola A, Difilippantonio MJ, Zhu J, Brown MJ, Tai X, Rogakou EP, Brotz TM, Bonner WM, Ried T and Nussenzweig A. (2000). *Science*, **290,** 1962–1965.

Dierov J, Prosniak M, Gallia G and Gartenhaus RB. (1999). *J. Cell Biochem.*, **74,** 544–550.

DiTullio Jr RA, Mochan TA, Venere M, Bartkova J, Sehested M, Bartek J and Halazonetis TD. (2002). *Nat. Cell Biol.*, **4,** 998–1002.

Duensing S and Munger K. (2002). *Oncogene*, **21,** 6241–6248.

Fernandez-Capetillo O, Chen HT, Celeste A, Ward I, Romanienko PJ, Morales JC, Naka K, Xia Z, Camerini-Otero RD, Motoyama N, Carpenter PB, Bonner WM, Chen J and Nussenzweig A. (2002). *Nat. Cell Biol.*, **4,** 993–997.

Furuta T, Takemura H, Liao ZY, Aune GJ, Redon C, Sedelnikova OA, Pilch DR, Rogakou EP, Celeste A, Chen HT, Nussenzweig A, Aladjem MI, Bonner WM and Pommier Y. (2003). *J. Biol. Chem.*, **278,** 20303–20312.

Hahn WC and Weinberg RA. (2002). *N. Engl. J. Med.*, **347,** 1593–1603.

Herbert GB, Shi B and Gartenhaus RB. (2001). *Oncogene*, **20,** 6777–6783.

Kang JS and Krauss RS. (1996). *Mol. Cell. Biol.*, **16,** 3370–3380.

Malumbres M and Barbacid M. (2001). *Nat. Rev. Cancer*, **1,** 222–231.

Morales JC, Xia Z, Lu T, Aldrich MB, Wang B, Rosales C, Kellems RE, Hittelman WN, Elledge SJ and Carpenter PB. (2003). *J. Biol. Chem.*, **278,** 14971–14977.

Paull TT, Rogakou EP, Yamazaki V, Kirchgessner CU, Gellert M and Bonner WM. (2000). *Curr. Biol.*, **10,** 886–895.

Petersen S, Casellas R, Reina-San-Martin B, Chen HT, Difilippantonio MJ, Wilson PC, Hanitsch L, Celeste A, Muramatsu M, Pilch DR, Redon C, Ried T, Bonner WM, Honjo T, Nussenzweig MC and Nussenzweig A. (2001). *Nature*, **414,** 660–665.

Prosniak M, Dierov J, Okami K, Tilton B, Jameson B, Sawaya BE and Gartenhaus RB. (1998). *Cancer Res.*, **58,** 4233–4237.

Rogakou EP, Boon C, Redon C and Bonner WM. (1999). *J. Cell Biol.*, **146,** 905–916.

Shi B, Hsu HL, Evens AM, Gordon LI and Gartenhaus RB. (2003). *Blood*, **102,** 297–302.

Stiff T, O'Driscoll M, Rief N, Iwabuchi K, Lobrich M and Jeggo PA. (2004). *Cancer Res.*, **64,** 2390–2396.

Wang H, Zeng ZC, Bui TA, Sonoda E, Takata M, Takeda S and Iliakis G. (2001). *Oncogene*, **20,** 2212–2224.

Ward IM and Chen J. (2001). *J. Biol. Chem.*, **276,** 47759–47762.

Ward IM, Minn K, Jorda KG and Chen J. (2003). *J. Biol. Chem.*, **278,** 19579–19582.